



**Chulalongkorn University**  
**The Ratchadaphisek Somphot Endowment Fund**

**Final Report**

**On**

**“Novel Synthesis Study of High Surface Area Silica”**

**By**

**Ms. Sujitra Wongkasemjit**

สถาบันวิจัยบริการ  
จุฬาลงกรณ์มหาวิทยาลัย

**March, 2002**

**Project Title** Novel Synthesis Study of High Surface Area Silica

**Name of the Investigator** Ms. Sujitra Wongkasemjit

**Month/Year Completed** March, 2002

### ABSTRACT

The sol-gel transition of tetra-coordinated spiro-silicate via hydrolysis and condensation under acidic and basic conditions is examined to elucidate the effect of catalyst, reaction time and temperature on the properties of obtained gel. The main advantage of this process is the low temperature employed, producing a solid network with a high specific surface area. FTIR spectroscopy and TGA analysis were used to characterize the formation of siloxane bonds (Si-O-Si). It is found that spiro-silicate can be hydrolyzed under both acid and base catalyzed conditions. The condensation rate to silicates is shown to be at a minimum in 1% of 1M HCl, which is the iso-electric point of silica. The prepared xerogel has a low-density and is an amorphous material with a specific surface area of 596 m<sup>2</sup>/g. Besides the catalyst media, the type of precursor also has a strong influence on the gel formation. An aminospio-silicate, six-membered ring, containing methyl and amino groups as substituents, was chosen for this study. The resulting xerogel is determined by the fact that to obtain the Si-O-Si bonds, a higher concentration of solvent and higher temperature are more favorable, due to the stability of the ring and branching of alkyl portion.

เลขที่	๘๐
เลขทะเบียน	๒๓ 15
เลขทะเบียน	๐๑๓๔๘
วัน,เดือน,ปี	๒๙ ต.ค. ๕๕

I 20378075

ชื่อโครงการ การศึกษาวิธีการสังเคราะห์ซิลิกาที่มีพื้นที่ผิวสูงแบบใหม่

ชื่อผู้วิจัย นางสุจิตรา วงศ์เกษมจิตร

เดือนและปีที่ทำวิจัยเสร็จ มีนาคม 2545

### บทคัดย่อ

การตรวจสอบแทนซิอันโซล-เจลของสไปโรซิลิเคตที่มีพื้นที่ผิวสูง โดยผ่านกระบวนการย่อยสลายด้วยน้ำ และการรวมตัวภายใต้สภาวะของความเป็นกรดและด่าง ปรากฏว่า คะตะลิสต์ที่ดี หรือ เวลาและอุณหภูมิที่ใช้ในการเกิดปฏิกิริยา มีผลต่อสมบัติของเจลที่ได้ ประโยชน์หลักของกระบวนการโซล-เจลนี้ คือ อุณหภูมิที่ใช้ในการเกิดเจลค่อนข้างต่ำ ซึ่งผลิตภัณฑ์ได้จากเจลจะมีพื้นที่ผิวที่สูง เครื่อง FTIR และ TGA เป็นเครื่องมือที่ใช้วิเคราะห์การเกิดพันธะซิล็อกเซน (Si-O-Si) จากการทดลอง พบว่า สไปโรซิลิเคตสามารถถูกย่อยสลายได้ด้วยคะตะลิสต์ที่มีสภาวะเป็นกรดหรือด่าง อัตราการเกิดซิลิเคตที่ดี เกิดที่สภาวะที่มีปริมาณกรดเกลืออยู่ 0.001 โมลาร์ (1% ของ 1M HCl) ซึ่งเป็นจุดไอโซอิเล็กทริกของซิลิกา ซิโรเจลที่เตรียมขึ้นมาได้มีความหนาแน่นต่ำ และเป็นวัสดุออสตรูมที่มีพื้นที่ผิวสูงถึง 596 ตารางเมตร ต่อ กรัม นอกจากนี้ปัจจัยของตัวคะตะลิสต์แล้ว ชนิดของสไปโรซิลิเคตก็มีอิทธิพลต่อการเกิดเจลเช่นกัน สารที่นำมาศึกษาในงานวิจัยนี้ คือ สารอะมิโนสไปโรซิลิเคต ซึ่งเป็นสารที่มีโครงสร้างเป็นวงแหวนหกเหลี่ยม และมีหมู่แทนที่สองหมู่ คือ กลุ่มเมทิล และกลุ่มอะมิโน ซิโรเจลที่เตรียมได้จากสารนี้ต้องใช้ความเข้มข้นของสารละลายคะตะลิสต์ และอุณหภูมิที่ใช้ในการเกิดปฏิกิริยาสูงกว่มาก สาเหตุเนื่องจากความเสถียรของวงแหวน และหมู่แทนที่ของสาร

## ACKNOWLEDGEMENT

The author would like to express her sincere appreciation to the Ratchadaphisek Somphot Endowment Fund, Chulalongkorn University, for financial support on this research work.



สถาบันวิทยบริการ  
จุฬาลงกรณ์มหาวิทยาลัย

**TABLE OF CONTENTS**

	<b>PAGE</b>
Title Page	i
Abstract (English)	ii
Abstract (Thai)	iii
Acknowledgement	iv
Table of Contents	v
List of Tables	vii
List of Figures	viii
<b>INTRODUCTION</b>	<b>1</b>
Sol-Gel Process of Silica-Type Materials	2
Advantages and Limitations of Sol-Gels	3
Polysiloxanes	3
Polycondensation of Polysiloxanes	4
Crosslinking Using Condensation Reaction	5
<b>OBJECTIVES</b>	<b>14</b>
<b>EXPERIMENTAL</b>	<b>15</b>
Materials	15
Equipment	16
Methodology	17
Synthesis of Tetra-Coordinated Spirosilicate, C <sub>2</sub> , from Silica and Ethylene Glycol	17
Synthesis of Aminospinosilicate, C <sub>4</sub> , from Silica and 2-Amino-2-methyl-1,3-propanediol	18
Sol-Gel Transition Study	18

	<b>PAGE</b>
Pyrolysis of Hydrolyzed Product	19
Density Measurement	19
<b>RESULTS AND DISCUSSION</b>	<b>20</b>
Synthesis	20
Sol-Gel Transition Study	24
Characterization of Pyrolyzed Spirosilicate C2	33
Characterization of Pyrolyzed Aminospinosilicate C4	38
Density Measurement	38
<b>CONCLUSIONS</b>	<b>40</b>
<b>REFERENCES</b>	<b>41</b>

สถาบันวิทยบริการ  
จุฬาลงกรณ์มหาวิทยาลัย

**LIST OF TABLES**

<b>TABLE</b>		<b>PAGE</b>
1	The FTIR bands of C2 and C4	20
2	The <sup>1</sup> H- and <sup>13</sup> C-NMR spectra of spirosilicate species	22
3	The pH results of different catalyst concentration	30
4	The ceramic yields of the hydrolyzed monomer after using 1M HCl at various gelation time	32
5	The BET surface area measurement of spirosilicate C2 after hydrolysis with 1% and 2% of 1M HCl at various time, followed by pyrolysis at 750°C for 7 h	34
6	The density measurement of pyrolyzed product C2 and fused silica (starting material)	38



สถาบันวิทยบริการ  
จุฬาลงกรณ์มหาวิทยาลัย

## LIST OF FIGURES

FIGURE		PAGE
1	A monolithic glass shapes made using the sol-gel process	4
2	Sketch of poly(dimethylsiloxane)PDMS chain, showing some structural information relevant to its high flexibility	4
3	Raman spectra obtained at various times during the sol-gel reaction in a solution containing 1:1:0.24 (vol) TMOS, MeOH, and $3 \times 10^{-3}$ M aqueous HCl	8
4	Schematics of silica gel network from the hydrolysis and condensation of TEOS; (A) acid and (B) base-catalyzed gel	10
5	Linear shrinkage versus temperature at $1^\circ\text{C}/\text{min}$ heating rate for silica gels prepared by three different methods. a) acid hydrolysis, b) base hydrolysis, c) colloidal process	12
6	Schematic of the synthesis of the tetra-coordinated spirosilicate	13
7	Schematic of the C2 tetra-coordinated spirosilicate synthesis	18
8	FTIR spectra of tetra-coordinated spirosilicates, a) C2 and b) amino, C4	21
9	$^1\text{H}$ -and $^{13}\text{C}$ -NMR spectra of tetra-coordinated spirosilicate, C2	22
10	$^1\text{H}$ -and $^{13}\text{C}$ -NMR spectra of aminospirasilicate, C4	23
11	TGA thermograms showing (%) weight loss due to thermal changes of tetra-coordinated a) spirosilicate, C2 and b) aminospirasilicate, C4	24
12	Schematic of hydrolysis and condensation under (a) hydrochloric acid solution and (b) ammonium hydroxide solution	25
13	FTIR spectra of hydrolyzed C2 monomer product with (a) 1% and (b) 2% of 1M HCl at room temperature	27



<b>FIGURE</b>		<b>PAGE</b>
14	FTIR spectrum of fused silica	27
15	The time-dependence of hydrolyzed products of spiro-silicate C2 with 1%-5% of 1M HCl at room temperature	28
16	FTIR spectra showing the effect of temperature on the hydrolyzed product	29
17	The time-dependence of hydrolyzed products of spiro-silicate C2 with 1%-4% of 1M NH <sub>4</sub> OH at room temperature	29
18	TGA thermograms showing percent ceramic yield at various times after hydrolysis with 1M HCl at (a) 1% and (b) 2%	31
19	FTIR spectra showing the effect of time on the hydrolyzed C4 product at 60°C	33
20	TGA thermogram showing percent ceramic yield of hydrolyzed aminospirosilicate, C4 at 60°C for 1, 3 and 4 h	33
21	SEM of hydrolyzed (a and b) and pyrolyzed (c and d) spiro-silicate C2	36
22	XRD patterns of pyrolyzed monomer and fused silica	37

## INTRODUCTION

Applications for sol-gel derived products are numerous. One of the largest application areas is for coatings and thin films used in electronic, optical, and electro-optic components and devices, such as substrates, capacitors, memory devices, infrared (IR) detection, and wave-guides. Moreover, the sol-gel method is also suitable for preparing catalytic materials. The term sol-gel was first coined in the late 1800s. The gel route to glasses and ceramics has been attractive in science and technology because of their diverse utilities (Turgay, 2000). Moreover, the sol-gel process offers new approaches to the synthesis of oxide materials. Starting from molecular precursors, such as metal alkoxides, an oxide network is obtained via inorganic polymerization reaction. Initiation is performed through the hydroxylation of metal alkoxides. As soon as hydroxyl groups are generated, propagation occurs through a polycondensation process. With an alkoxide ( $M(OR)_n$ ) as a precursor, sol-gel chemistry can be described in terms of two classes of reactions: (David, 1995; Charles, 1994)

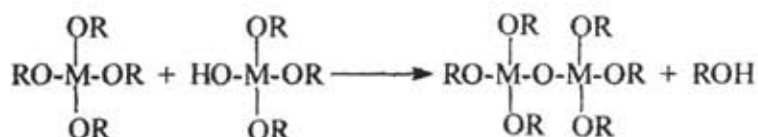


**Condensation:**

(a) Dehydration



(b) Dealcoholation



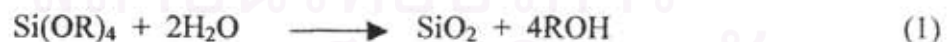
In fact, sol-gel chemistry generally refers to a low temperature method using chemical precursors that can produce more pure and homogenous materials than

conventional high temperature processes. The low temperature method leads to the formation of oxides with amorphous that are difficult to prepare by other methods.

Sol-gel chemistry of silicon alkoxides is rather simple, compared to that of complexes of transition metal alkoxides in which metal atoms may exhibit several coordination states. Molecular precursors of silicon alkoxides are always monomeric tetrahedral species  $\text{Si}(\text{OR})_4$ . One of the usual starting materials for silica glasses is tetraethylorthosilicate (TEOS,  $\text{Si}(\text{OCH}_2\text{CH}_3)_4$ ) (Turner, 1986 ). However, many other alkoxide precursors can be used to impart different properties to the gels. Recently, an inexpensive method of silica has been developed into precursors called glycolato silicate species, which produces refined powders. The advantages of these species are low cost, easy process and environmental friendly (Varangkana, 2001). By applying the sol-gel method, the resulting xerogel exhibited different chemical properties, which is evidenced by the step-growth polymerization determined by solvent content, acid or base, aging time and temperature.

### Sol-Gel Process of Silica-Type Materials

Silicon containing materials are derived from the synthesis of oxides involving hydrolyzable alkoxides that undergo a sol-gel transition. The sol-gel transition represents a linking of nanometer-sized units, around  $100\text{\AA}$ , into an oxide network of infinite molecular weight. The process involves polymerization and branching, but a typical overall reaction may be written as eq. 1



Where the  $\text{Si}(\text{OR})_4$  organometallic species is typically TEOS. In this application, the organometallic compound is hydrolyzed, condensed to polymeric chains, the chain becomes more and more branched, and finally a highly swollen gel is formed. It is first dried at moderately low temperatures to remove volatile species, and then is fired into a porous ceramic object.

## Advantages and Limitations of Sol-Gels

The advantages of the sol-gel process in general are;

- a higher purity of starting materials is obtained,
- a relatively low temperature is required, reducing loss of volatile components,
- the possibility of controlling the "ultra-structure" of the ceramic (to reduce the microscopic flaws that lead to brittleness) results, and
- ceramic coatings can be formed.

The disadvantages of sol-gel processing include the shrinkage of the ceramics from removal of the solvents and the need for expensive high-purity alkoxides. This tends to limit the use of the process for bulk ceramics, but is a minor factor for specialty applications or those cases where conventional technology fails.

## Polysiloxanes

The Si-O backbone of this class of polymers endows it with a variety of intriguing properties. The strength of these bonds gives the siloxane polymers considerably thermal stability, which is important for their use in high temperature applications, for examples, as heat-transfer agents and high-performance elastomers. The nature of the bonding and the chemical characteristics of the side groups give the chains a very low surface energy and therefore, highly unusual and desirable surface properties.

Several structural features make the siloxane backbone one of the most flexibles in all of polymer science. The reasons for this extraordinary flexibility can be seen in Figure 1. First, because of the nature of the bonding, the Si-O skeletal has a bond length of 1.64 Å which is significantly larger than that of the C-C bond (1.53 Å) found in most organic polymers.



**Figure 1** A monolithic glass shapes made using the sol-gel process.

As a result, steric interferences or intramolecular congestion is diminished. The oxygen skeletal atoms are also unencumbered by side groups, and still have the divalency needed to continue a chain structure. Finally the Si-O-Si bond angle ( $180-\theta'$ ) of  $\approx 143^\circ$  is much more open than the usual tetrahedral bonding ( $\approx 110^\circ$ ), and torsional rotations can occur without incurring a serious energy penalty (Figure 2).

These structural features have the effect of increasing the dynamic flexibility of the chain (James, 1992).

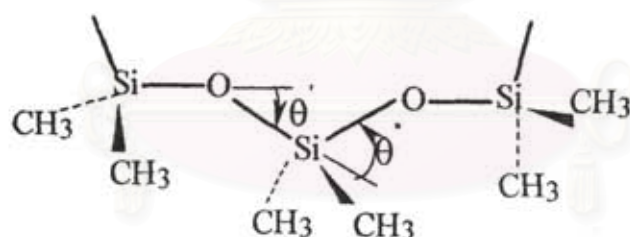
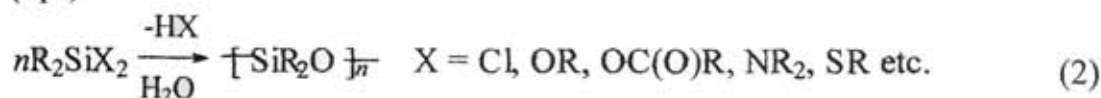


**Figure 2** Sketch of poly(dimethylsiloxane), PDMS, chain, showing some structural information relevant to its high flexibility.

### Polycondensation of Polysiloxane

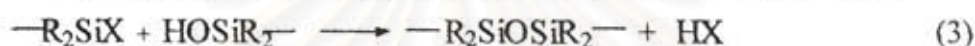
Polycondensation processes are often applied for the synthesis of both linear siloxane polymers and cyclic siloxane oligomers. A polysiloxane chain is most often formed as a result of two types of polycondensation; homofunctional polycondensation of silanediols and heterofunctional polycondensation involving the silanol group and another function. These reactions usually constitute the second step of the hydrolytic

polycondensation of organosilanes having two hydrolyzable groups attached to silicon (eq.2).



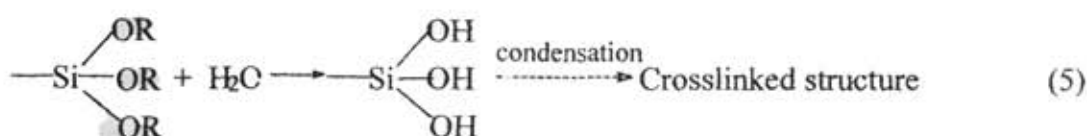
Both steps, hydrolysis and polycondensation, usually occur in one process. If the hydrolysis is much faster and an excess of water is used, then the silane is fully transformed into silanediol and the polymer is formed from the homofunctional silanediol polycondensation.

Heterofunctional polycondensation (eq.3) is favored in the process of eq.2 when the functional group is less reactive and a limited amount of water is used.



### Crosslinking Using Condensation Reactions

The condensation of silanol to form siloxane bonds (eq.4) is a reaction of considerable importance in industrial silicone chemistry. If it were feasible to extend this chemistry to molecules where more than one silanol group is attached to a single silicon atom, then this condensation reaction could be used to produce a three-dimensional crosslinked matrix with the desirable absence of any additional organic character, except siloxane bonds (eq.5). The principle, however, has been harnessed successfully in room temperature curing systems. Molecules are synthesized (which contain  $=Si(OR)_2$  or  $-Si(OR)_3$  groups) as part of the siloxane chain and these groups, on exposure to atmospheric moisture, are spontaneously hydrolyzed and condensed to give a three-dimensional crosslinked network.



If we include the initial hydrolysis of the  $-OR$  functional group attached to

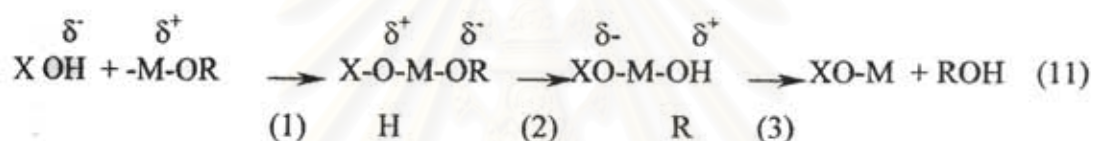


attack. Their reaction with XOH molecules containing reactive hydroxy groups can be written as follows;



Depending on the chemical nature of X, such a reaction corresponds to hydrolysis (X = H), condensation (X = M). An associative nucleophilic substitution could be described following a 3 step process:

- Nucleophilic addition of the XOH group onto the positively charged metal atom.
- Proton transfer, within the transition state  $M(OR)_n(XOH)$  from the entering molecule to the leaving alkoxy group.
- Departure of the positively charged protonated species.



The whole process depends on charge distribution in the alkoxide and the transition state  $(HOX)-M-(OR)_n$ . Basically, the metal atom M and the leaving group ROH have to be positively charged.

In the study of the reactivity of tetramethylorthosilicate (TMOS) towards gelation, Lippert et al. (1988) were able to assign eight of the Raman bands observed during the gelation of TMOS. Figure 3 shows the Raman spectrum with a band at  $646 \text{ cm}^{-1}$  due to TMOS at early times together with bands at  $673$ ,  $696$  and  $726 \text{ cm}^{-1}$  (due to hydrolysis products). A strong broad band due to dimer also appears at early times at  $609 \text{ cm}^{-1}$ . The bands on the high frequency side of TMOS disappear rapidly and the band at  $609 \text{ cm}^{-1}$  becomes dominant but with a shoulder at  $589 \text{ cm}^{-1}$ . At later times these bands give way with sequential growth and conversion of multimeric bands at  $525$ ,  $484$  and  $432 \text{ cm}^{-1}$ .



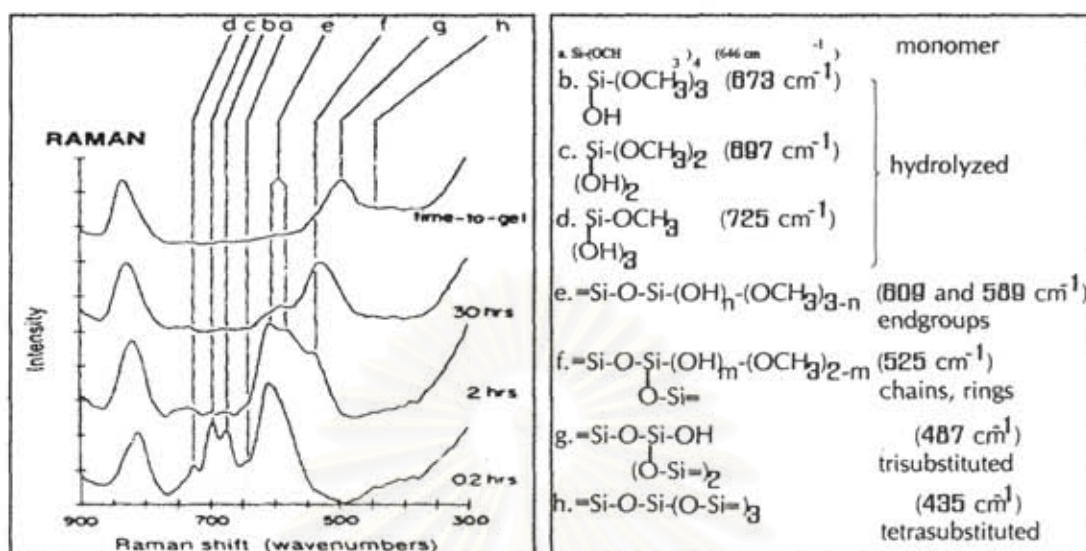
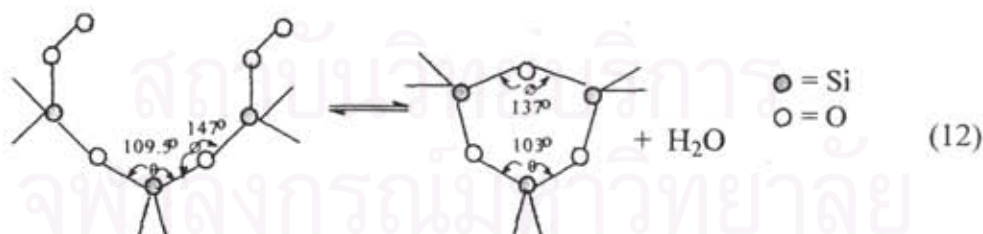


**Figure 3** Raman spectra obtained at various times during the sol-gel reaction in a solution containing 1:1:0.24 (vol) TMOS, MeOH, and  $3 \times 10^{-3}$  M aqueous HCl. (Lippert et al. (1988)).

In the same year Brinker et al. (1988) observed that the formation of a cyclic trisiloxane are absent in the as-dried gel. These species form at intermediate temperatures predominantly on the silica surface by the condensation of isolated vicinal silanol groups located on unstrained precursors via the following reaction;



The heat of formation of 3-membered rings according to reaction (12) is calculated to be quite endothermic ( $\Delta H_f = 23 \text{ kcal/mole}$ ). This is due to the strain energy required to reduce the bond formation ( $\text{O-Si-O}$ ) to  $136.7^\circ$  from its equilibrium value,  $147^\circ$ , and to reduce the tetrahedral ( $\text{O-Si-O}$ ) angle to  $103.3^\circ$  from  $109.5^\circ$ .

The altered environments of siloxane bonds contained within tri-siloxane greatly influence their stability. The changes in tetrahedral symmetry around silicon activate empty d-acceptor orbitals, making Si more acidic. By decreasing bond formation ( $\emptyset$ ), transfer electron density into the lone pair orbitals of the bridging oxygen makes the oxygen more basic and the silicon more acidic. The increased polarity and enhanced acid/base properties of strained Si-O bonds promote the adsorption of water on the bond and the subsequent bond hydrolysis reaction (the reverse of eq.13), according to the following mechanism.



The classic example of using sol-gel kinetics to control the pore structure of products is the effect of pH on the properties of silica. Under acid conditions hydrolysis occurs at a faster rate than condensation and the resulting gel is weakly branched. Condensation is accelerated relative to hydrolysis with increasing pH. Thus, a base-catalyzed gel is highly branched and contains colloidal aggregates. Handy et al. in 1991 (David et al. (1995)) found that because of the different extent of branching, acid-catalyzed gels contain mostly micropores whereas base-catalyzed ones contain mesopores. There are also chemical differences. Ying et al. in 1992 and 1993 (David et al. (1995)) have shown that acid-catalyzed gels contain higher concentration of silanol groups than base-catalyzed ones, as shown in figure 4.

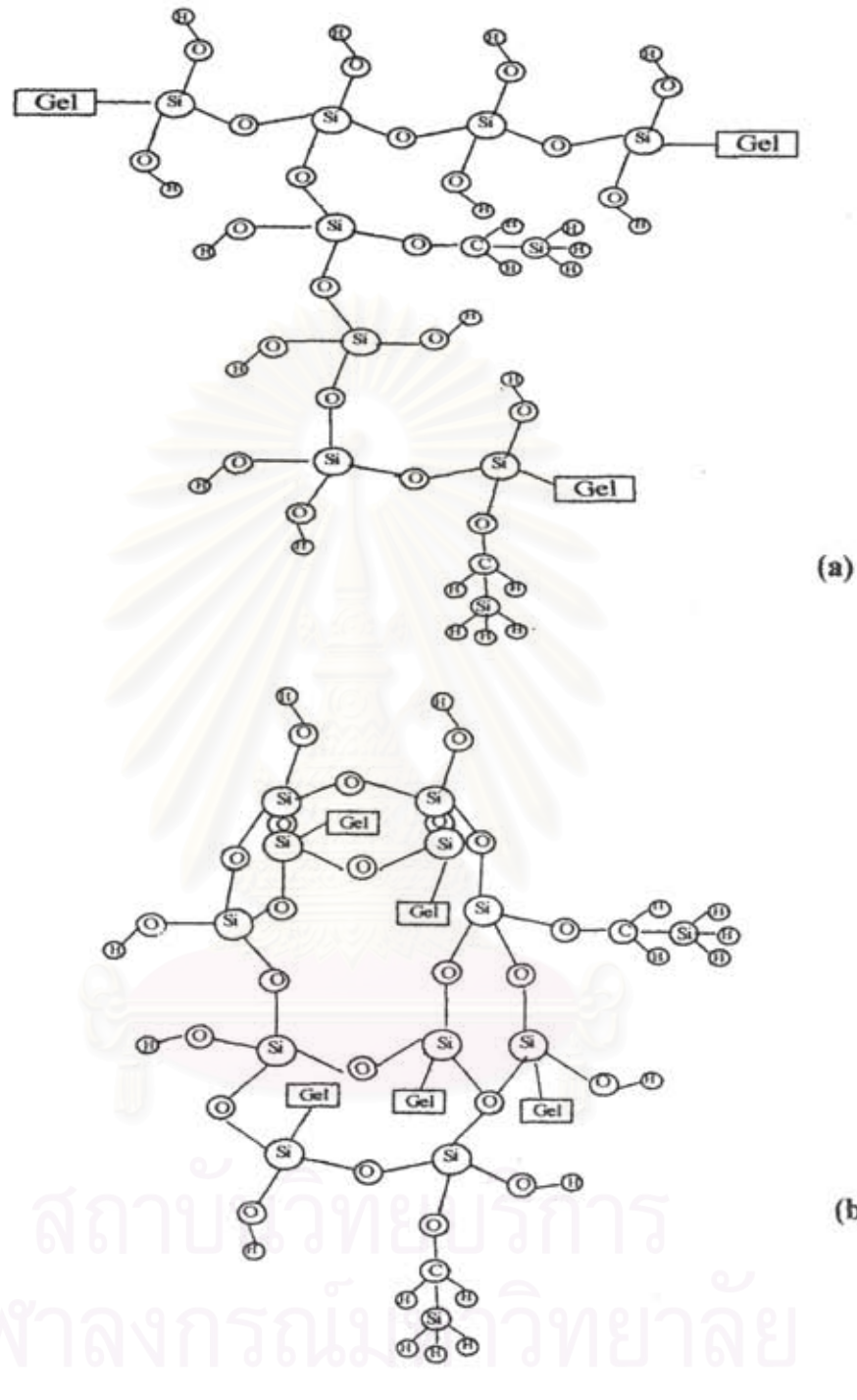


**Figure 4** Schematics of silica gel network from the hydrolysis and condensation of TEOS; (a) acid and (b) base-catalyzed gel. (David et al. (1995))

Another important parameter that affects a sol-gel product is the type of precursor. It was found that the size of the alkoxy ligands changes the rates of both hydrolysis and condensation due to steric and inductive effects (David, 1995).

Charles (1994) suggested that by having formed gel, conversion to an inorganic oxide structure is accomplished by heat treatment. The behavior of a gel on heating can be considered in three parts:

1. Drying and pyrolysis of organics
2. Structural rearrangement and densification
- and 3. Crystallization.

Differences in the drying behavior and in the physical properties of gels can be explained in terms of the different structural rearrangements that occur on removal of the solvent. Two extremes of gel structure: linear polymeric chains formed under (say) acidic conditions, and a highly cross-linked colloidal gel formed (for example) in a basic environment are considered. Owing to the low levels of cross-linking in acidic low-water gels, considerable structural rearrangement can occur, resulting in high density, low pore volume gels. With greater water addition, or under basic conditions, structural rearrangements still occur, but due to the already highly cross-linked nature of the gel, less densification is possible, and larger pore volume results.

Brinker (1988) investigated the formation of gels towards dense glasses and ceramics by thermal treatments, causing a second stage of shrinkage. Owing to the very high surface areas and very small pore dimensions, gels may be completely densified at such low temperatures, as shown in figure 5.

As a consequence, much effort is devoted to the understanding of the sol-gel transition using a variety of experimental techniques.

Charoenpinijkarn (2001) studied the sol-gel processing of polysilatrane. It was observed that high pH solution accelerates the hydrolysis rate, resulting in fast gelling time. Additionally, after gelation has occurred the reaction continues since the cross-linking is not yet completed in this step, leaving some organic ligand. The pure  $\text{SiO}_2$  network is obtained by pyrolyzing the gel to  $800^\circ\text{C}$  to remove all organic ligands.

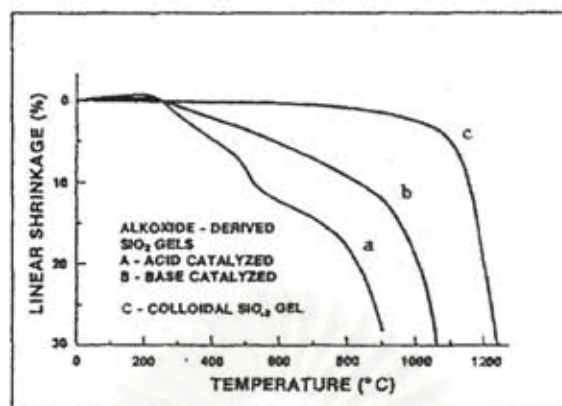


**Figure 5** Linear shrinkage versus temperature at  $1^{\circ}\text{C}/\text{min}$  heating rate for silica gels prepared by three different methods: a) acid hydrolysis, b) base hydrolysis, c) colloidal process. (Brinker et al. (1990))

Varangkara (2001) successfully synthesized spirosilicates from  $\text{SiO}_2$  and ethylene glycol, EG, and ethylene glycol derivatives in the presence of triethylenetetramine, TETA, as a base or catalyst, with/without potassium hydroxide, KOH, as a co-catalyst, as shown in figure 6, where R represents as

- i).  $-\text{CH}_2\text{CH}_2-$
- ii).  $-\text{CH}_2(\text{CH}_3)\text{C}(\text{NH}_2)\text{CH}_2-$

สถาบันวิทยบริการ  
จุฬาลงกรณ์มหาวิทยาลัย

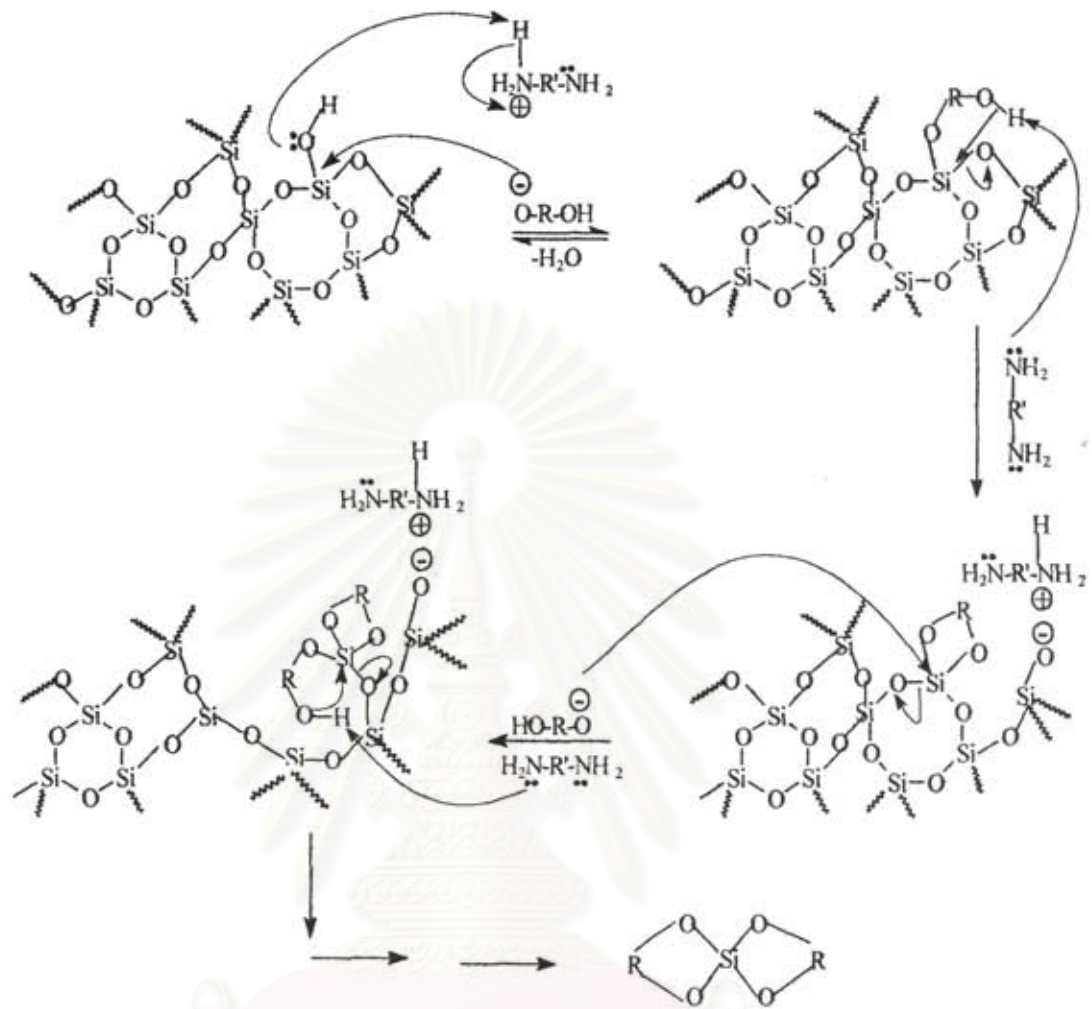


**Figure 6** Schematic of the synthesis of the tetra-coordinated spirosilicates.

สถาบันวิทยบริการ  
จุฬาลงกรณ์มหาวิทยาลัย

## OBJECTIVES

- To study the effect of reaction conditions on the kinetics of C2 and C4 sol-gel transition.
- To study the optimal conditions to high surface area silica for further use in many applications.



สถาบันวิทยบริการ  
จุฬาลงกรณ์มหาวิทยาลัย

## EXPERIMENTAL

### Materials

Fused silicon dioxide or HI-SIL 927 silica ( $\text{SiO}_2$ ), with a surface area of  $168 \text{ m}^2/\text{g}$ , by BET, was donated by PPG Siam Silica Co., Ltd. Fumed silicon dioxide with a surface area  $320 \text{ m}^2/\text{g}$  was purchased from Aldrich Chemical Company. Both Fused and Fumed silicon dioxide were dried in oven at  $100^\circ\text{C}$  for 10 h.

2-amino-2-methyl-1,3-propanediol ( $\text{HOCH}_2\text{C}(\text{CH}_3)(\text{NH}_2)\text{CH}_2\text{OH}$ ) was purchased from Aldrich Chemical Company, used without purification and kept under nitrogen atmosphere.

Ethylene glycol (EG,  $\text{HOCH}_2\text{CH}_2\text{OH}$ ), purchased from Labscan, was used as a reaction solvent. It was distilled by fractional distillation at  $200^\circ\text{C}$  under  $\text{N}_2$  atmosphere. Triethylenetetramine [TETA,  $\text{H}_2\text{N}(\text{CH}_2\text{CH}_2\text{NH})_3$ ] was purchased from Facai Polytech Co., Ltd., used as received and as a catalytic base. It was purified by vacuum distillation at  $120^\circ\text{C}$  (0.1 mmHg).

Potassium hydroxide (KOH) was purchased from Baker Analyzed Reagent. It was used as received as catalyst.

Methanol ( $\text{CH}_3\text{OH}$ ) and acetonitrile ( $\text{CH}_3\text{CN}$ ) were purchased from Baker Analyzed Reagent and Lab-scan Analytical Science. They were used as precipitating agents and purified by fractional distillation under nitrogen gas over magnesium activated with iodine and calcium hydride, respectively. Both were stored over molecular sieves.

Hydrochloric acid solution (HCl) and ammonium hydroxide solution ( $\text{NH}_4\text{OH}$ ) were diluted with deionized water at various concentrations. They were used as an electrolyte.

UHP grade nitrogen gas with 99.99% purity was purchased from Thai Industrial Gases Public Company Limited (TIG).



## Equipment

### 1. Fourier Transform Infrared (FTIR) Spectroscopy

FTIR spectra were obtained on a Vector 3.0 Bruker Spectrometer with 32 scans at a resolution of  $4\text{ cm}^{-1}$ . A frequency range of  $4000\text{--}400\text{ cm}^{-1}$  was observed using a deuterated triglycinesulfate detector (DTGS) with specific detectivity of  $D^* = 1 \times 10^9\text{ cm} \times \text{Hz}^{1/2} \times \text{W}^{-1}$ . The powder samples were pressed to form pellets by mixing with pure and dry crystalline potassium bromide, KBr.

### 2. Nuclear Magnetic Resonance Spectroscopy (NMR)

$^1\text{H}$  and  $^{13}\text{C}$ -NMR spectra were obtained on a 200 MHz JEOL spectrometer at the Chemistry Department, Faculty of Science, Chulalongkorn University at room temperature. While  $^{29}\text{Si}$ -NMR spectra were obtained on 500 MHz JEOL spectrometer at the Scientific and Instrument Research Equipment Centre, Chulalongkorn University. Deuterated dimethyl sulfoxide ( $\text{DMSO-d}_6$ ) was used as a solvent. Tetramethylsilane (TMS) was used as the reference.

### 3. Thermogravimetric Analysis (TGA)

TGA measurement data were obtained on a Du Pont instrument, Du Pont TGA 2950, using a platinum pan, using samples of 12-15 weight. The temperature program was started from room temperature to  $750^\circ\text{C}$ , with a heating rate of  $10^\circ\text{C}/\text{min}$  and nitrogen flow rate of  $25\text{ mL}/\text{min}$ .

### 4. Scanning Electron Microscope (SEM)

SEM digitized micrographs were obtained from a JEOL 5200-2AE (MP 15152001) scanning electron microscope with magnification range of  $35\text{--}20,000\times$ . Micrographs of the sample surfaces were obtained using a voltage  $25\text{ kV}$  at  $5000$  and  $7500$  magnification. The pyrolyzed samples were stuck to aluminium stubs. Before characterization, these stubs with samples were dried in vacuum oven at  $60^\circ\text{C}$  and kept in silica gel-container before coated with gold by vapor deposition.

### 5. BET Surface Area Measurement

Surface area of pyrolyzed product was determined by Autosorb-1 Gas sorption system (Quantachrome Corporation) with the Brunauer-Emmett-Teller method (BET). A gaseous mixture of nitrogen and helium was allowed to flow through the system at a constant rate of  $30\text{ ml}/\text{min}$ . The nitrogen gas was injected with

a one milliliter syringe to calibrate the analyzer for each gas composition and also used as the adsorbate at liquid nitrogen temperature. Each sample was degassed at 300°C for 3 h before measurement. The surface area of the samples was obtained from five point adsorption. The results were calculated based on the desorption surface area and the dried weight of the sample after analysis.

#### 6. Wide Angle X-Ray Diffractometer (WXR)

WXR used in this study was D/MAX 2000 series of Rigaku X-ray Diffractometer system. X-ray of Cu k-30 mA was used as a source. The k-beta filter was used to eliminate interference peak. Divergence slit and scattering slit at 1 degree together with 0.3 mm of receiving slit were set. The experiment was performed in the range of 5-90 degree with scan speed 5 deg/min and 0.02 degree for scan step.

### **Methodology**

#### ***Synthesis of Tetra-Coordinated Spirosilicate, C2, from Silica and Ethylene Glycol***

The reaction mixture was prepared according to Varangkana's work (2001) in a round bottom flask at room temperature. Powder of fused silica (6g, 0.1mol) was dissolved in excess of ethylene glycol (20 ml), resulting in clear solution. Afterwards triethylenetetramine (18.24g, 0.12mol) was quickly added. The reaction was carried out under nitrogen atmosphere at the boiling point of ethylene glycol. The mixture was heated to distill off EG and by-product water, see figure 7. The mixture turned to yellow clear in 24 h and was then allowed to stand at room temperature to cool down. The solution mixture was purified using 10% of distilled methanol in 90% of distilled acetonitrile. The white powder product was stored in a silica gel container due to the moisture absorption property.

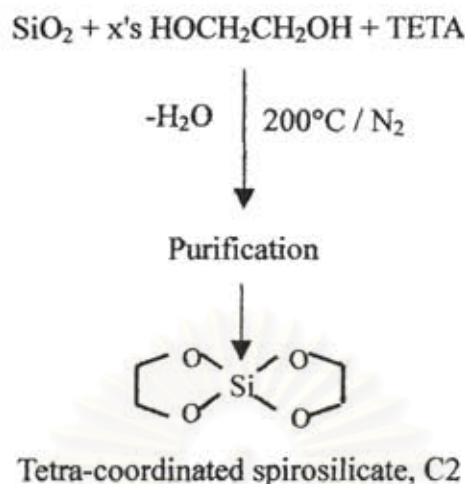
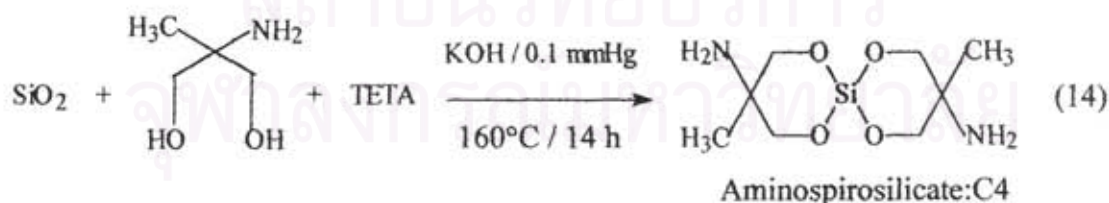


**Figure 7** Schematic of the C<sub>2</sub> tetra-coordinated spirosilicate synthesis.

***Synthesis of Aminospirosilicate, C4 from Silica and 2-Amino-2-methyl-1,3-propanediol***

The product of aminospirosilicate, C4 (Varangkana, 2000) was prepared in a round bottom flask at room temperature with a mixture of 0.033 mol (2 g) fumed silica, 50 mL of TETA, 0.2 mol (21 g) 2-amino-2-methyl-1,3 propanediol, and 7 mol percent of KOH equivalent to silica. The reaction was carried out at 160°C under vacuum, 0.1 mmHg, for 14 h, see eq.14, to obtain TETA and water as by-product. The mixture was then allowed to cool down, precipitated by using 10% of distilled methanol in 90% of distilled acetonitrile. The white powder product was kept in silica gel container due to the moisture absorption property.



***Sol-gel Transition Study***

Hydrolysis of the synthesized C2 and C4 tetra-coordinated spirosilicates was carried out by addition of either HCl or NH<sub>4</sub>OH solution at various concentrations. The

mixture was prepared directly in 7 in. crucible at room temperature, resulting in a formed-gel product, afterwards the gel was aged at room temperature. To study the sol-gel transition, at each hour the aliquots of mixture were deducted and dried using high vacuum (0.1 mmHg) to remove solvent. The hydrolysis reaction was also carried out at 40° and 60°C.

### *Pyrolysis of Hydrolyzed Product*

The hydrolyzed gels obtained from previous sections were pyrolyzed in a furnace at a heating rate of 10°C/min to 750°C and temperature maintained at 750°C, for 7 h. The pyrolyzed products were then characterized using TGA, FTIR, BET, SEM and WXRd.

### *Density Measurement*

The volumetric property of the monomer C2, the stable hydrolyzed product from 3.3.3, was determined using a 25 mL pycnometer (for powder form product) and distilled isooctane as media. The measurement was performed at 25°C. The purified product in the bottle was weighed in the range of 0.5-1.0 g. The media was added until covering the product. Then the bottle was sonicated and incubated at 25°C for 2 h before adding the media to the marked point. The same procedure was made with fused silica for comparison.

สถาบันวิทยบริการ  
จุฬาลงกรณ์มหาวิทยาลัย

## RESULTS AND DISCUSSION

### *Synthesis*

The synthesized product of tetra-coordinated spirosilicate, C2, and aminospirosilicate, C4, were prepared following Jitchum's work. The products were identified using FTIR, NMR and TGA, as described following.

#### Fourier Transform Infrared (FTIR) Spectroscopy

The white powder products of tetra-coordinated spirosilicates, C2, and aminospirosilicate, C4, were characterized by mixing with KBr, as shown in figure 8. The characteristic peaks of each product are summarized in table 1.

**Table 1** The FTIR bands of C2 and C4.

Products	Functional groups	Wave number (cm <sup>-1</sup> )
Monomer :C2	O-H stretching	Broad band at 3405 cm <sup>-1</sup>
	C-H stretching	2951-2883 cm <sup>-1</sup>
	Si-O-CH stretching (Jitchum,2000)	1086, 944, and 883 cm <sup>-1</sup>
Monomer :C4	O-H stretching	Broad band at 3405 cm <sup>-1</sup>
	C-H stretching	2951-2883 cm <sup>-1</sup>
	Si-O-CH stretching (Jitchum,2000)	1086 and 944 cm <sup>-1</sup>

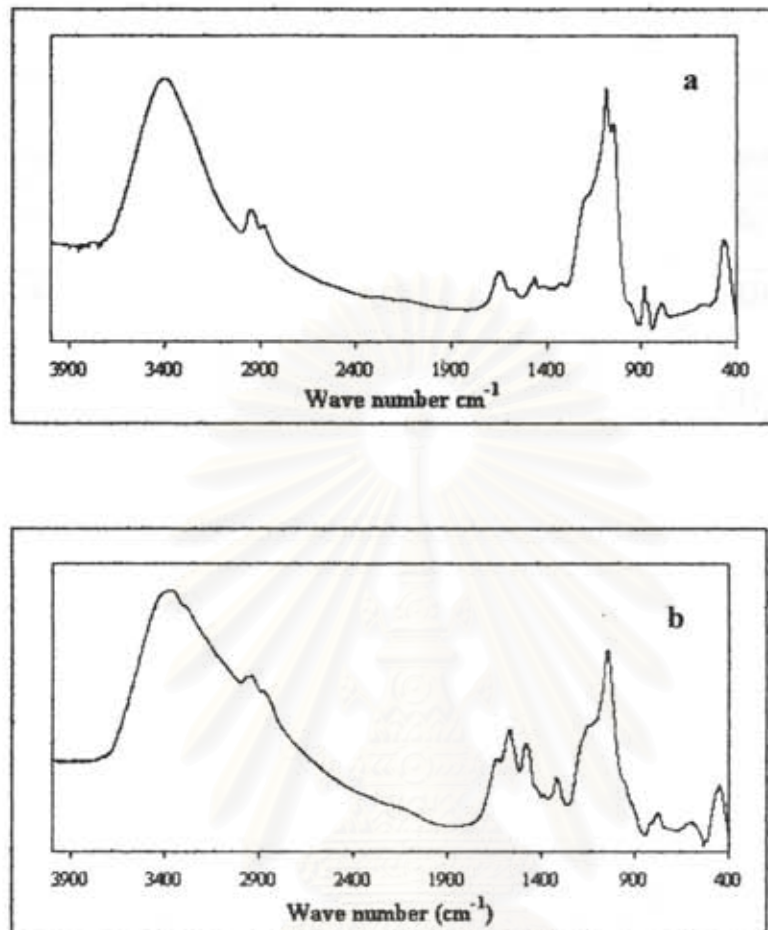


**Figure 8** FTIR spectra of tetra-coordinated spiro-silicates, a) C2 and b) amino, C4.

Proton and Carbon Nuclear Magnetic Resonance Spectroscopy  
( $^1\text{H}$ - and  $^{13}\text{C}$ -NMR)

The spectra of  $^1\text{H}$ - and  $^{13}\text{C}$ -NMR of tetra-coordinated spiro-silicates, C2 and amino C4, are shown in figures 9 and 10, respectively. The results are summarized in table 2.

**Table 2** The  $^1\text{H}$ - and  $^{13}\text{C}$ -NMR spectra of spiro-silicate species.

Type of products	Chemical shift (ppm)		Assignment
	$^1\text{H}$ -NMR	$^{13}\text{C}$ -NMR	
Monomer :C2	3.27	62.75	$\text{CH}_2\text{-O}$
Monomer :C4	0.83	22.11	$\text{CH}_3$
	-	53.47	$\text{C}$
	3.13	67.12	$\text{CH}_2\text{-O}$

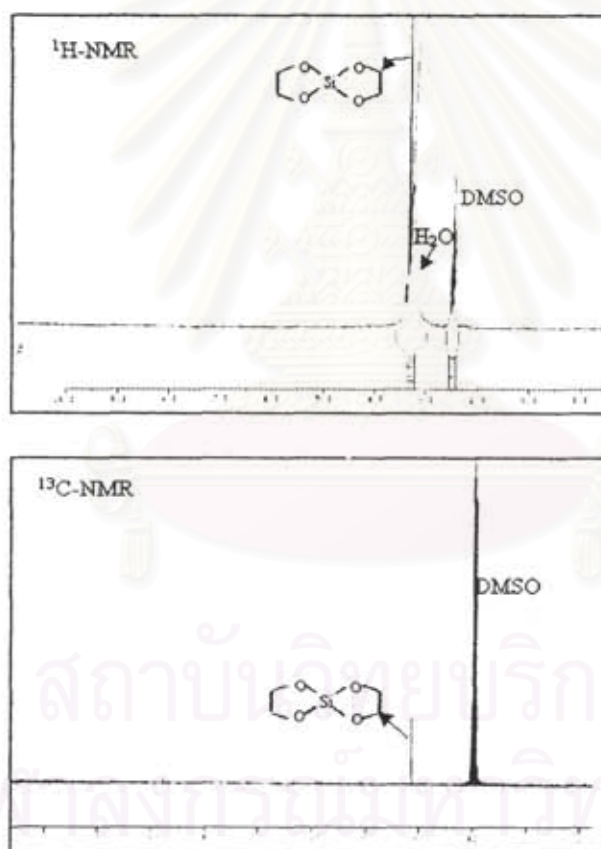


**Figure 9**  $^1\text{H}$ - and  $^{13}\text{C}$ -NMR spectra of tetra-coordinated spiro-silicate, C2.

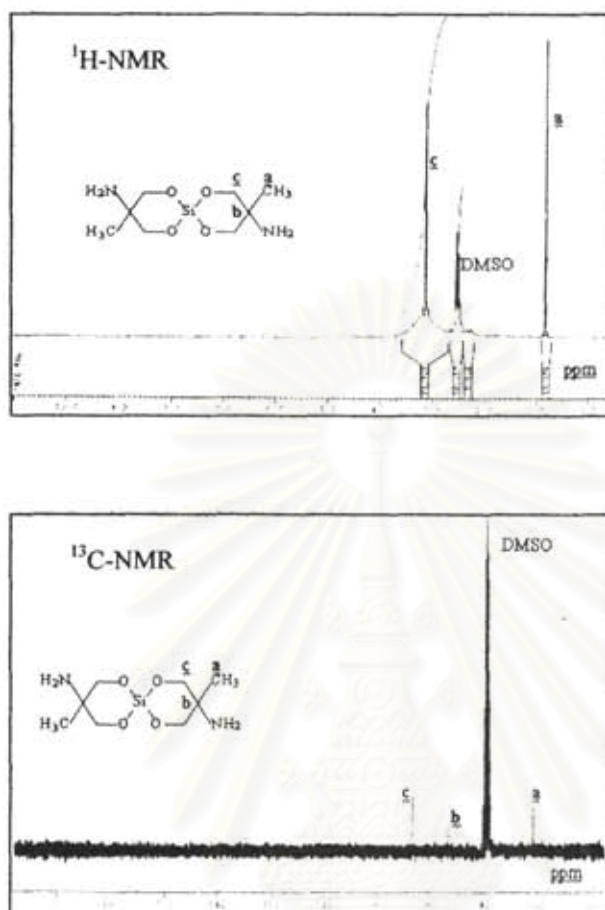


**Figure 10**  $^1\text{H}$ - and  $^{13}\text{C}$ -NMR spectra of aminospirosilicate, C4.

#### Thermogravimetric Analysis (TGA)

The result of TGA, as indicated in figure 11, gave the final ceramic yields for monomers C2 and C4 42.74%, and 26.84%, respectively. The theoretical yields of both are 40.05% and 25.64%, respectively. The differences are due to the further crosslinking of the monomers during heating since the final residue was black.

FTIR, NMR and TGA results indicated that the spirosilicates were successfully synthesized.



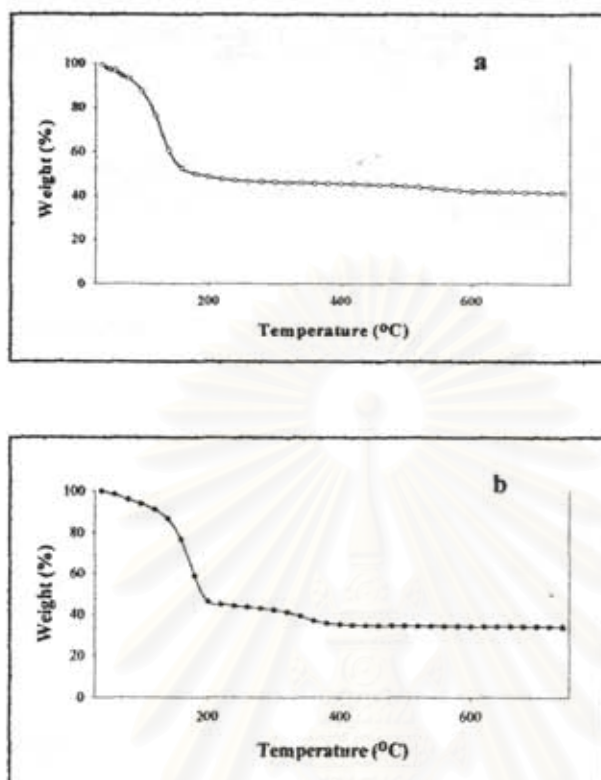
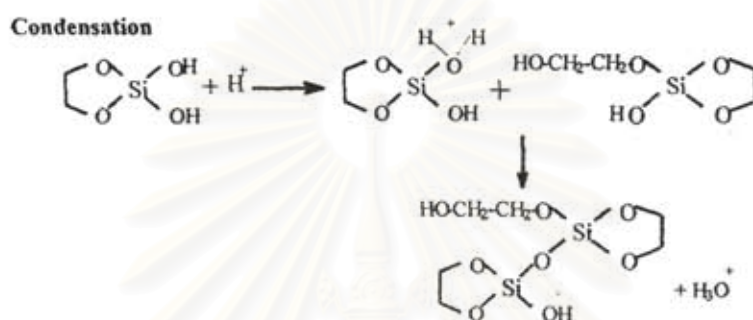
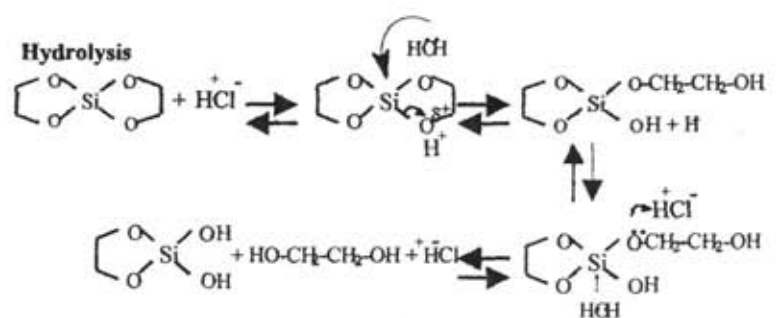


**Figure 11** TGA thermograms showing (%) weight loss due to thermal changes of tetra-coordinated a) spirosilicate, C2 and b) aminospirosilicate, C4.

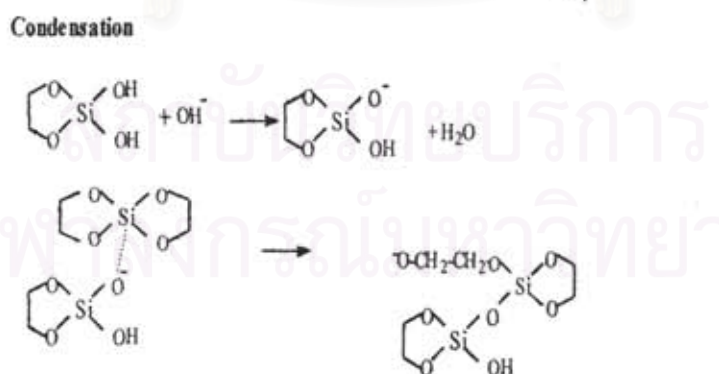
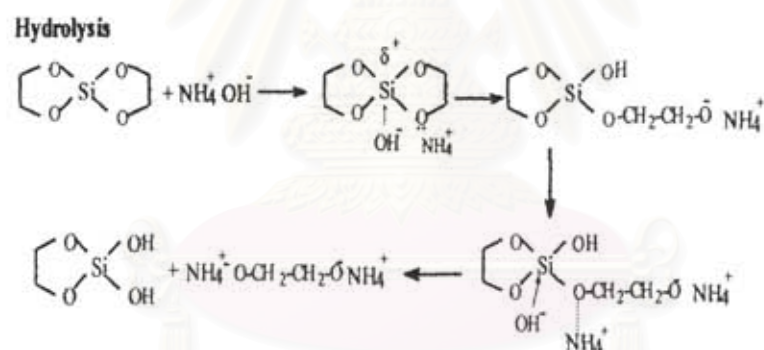
### *Sol-gel Transition Study*

It is well known that the catalyst used in a gelation reaction can have large effects on the microstructure of the gels formed as well as on the rapidity of the gelation process (Mackenzie, 1986). During sol to gel transition induced by applying solvent, the polymerization occurs via hydrolysis and polycondensation reaction. Figure 12 shows two proposed mechanisms of hydrolysis and condensation for tetracoordinated spirosilicates under acidic and base conditions.

The hydrolyzed products of monomer C2 and C4 were identified using FTIR and TGA, as described below.



(a)



(b)

**Figure 12** Schematics of hydrolysis and condensation under (a) hydrochloric acid solution and (b) ammonium hydroxide solution.

*Tetracoordinated spirosilicate C2*Fourier Transform Infrared (FTIR) Spectroscopy : Using 1M hydrochloric acid solution

It is worth noting that using less than 1% of 1M HCl, spirosilicate C2 can not form gel within one week. The main reason probably comes from not enough proton species to hydrolyze the starting material.

From figure 13 (a) using 1% of 1M HCl, it was shown that the characteristic peaks at 3405, 2951, 2883, 1086 and 883  $\text{cm}^{-1}$  decreased as the time increased. The decrease in the absorption at 3405  $\text{cm}^{-1}$  was attributed to the decrease in the amount of Si-OH due to the condensation of silanols (Yamane, 1988). At the same time, the absorption peak around 1648  $\text{cm}^{-1}$ , which was assigned to the OH bending (Jung, 2000), also decreased in the same manner. The change in the absorption peak at 1086  $\text{cm}^{-1}$  suggests that crosslinking of Si-O-Si bonds occurs via hydrolysis and condensation. This was confirmed by comparison with the disappearance of absorption peaks at 3405, 2951, 2883  $\text{cm}^{-1}$ , indicating a decrease of organic groups (carbon atom). It should be noted that at 9 h the absorption peaks at 3405, 2951, 2883, 1086 and 883  $\text{cm}^{-1}$  were changed in reverse direction (Brinker, 1988, 1990), and further decreased again at 10 h and obtained the final result at 11 h.

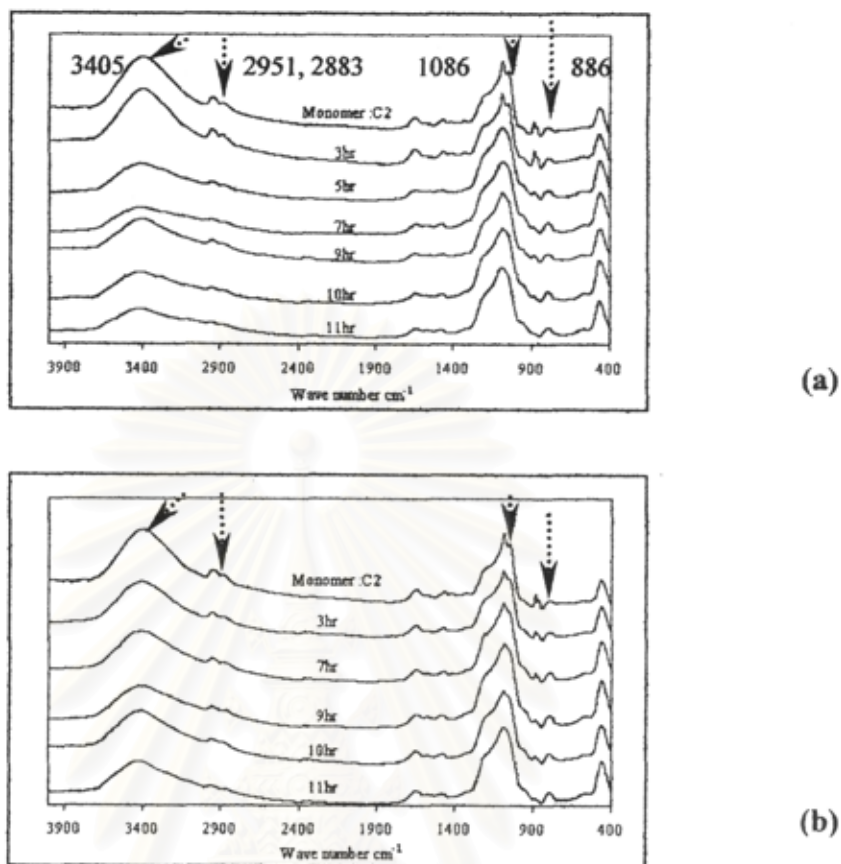


**Figure 13** FTIR spectra of hydrolyzed C2 monomer products with (a) 1% and (b) 2% of 1M HCl at room temperature.

The structure at this point of hydrolyzed products obtained was very close to that of silica. The FTIR structure of fused silica is shown in figure 14.

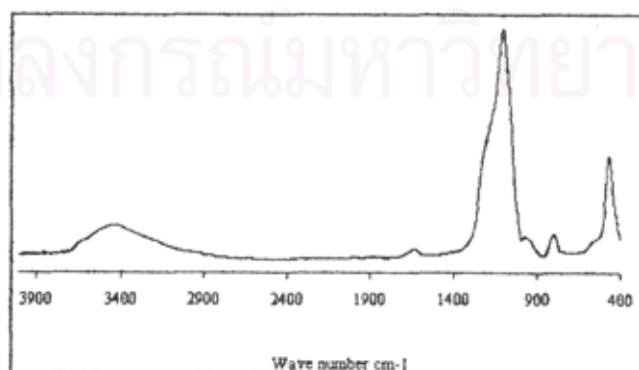


**Figure 14** FTIR spectrum of fused silica.

From figure 13 (b) for 2% of 1M HCl, the obtained results were almost the same as figure 12 (a). In addition, the change of absorption peaks at 3405, 2951, 2883, 1086 and 886  $\text{cm}^{-1}$  initially decreased faster in the beginning when compared to lower concentration of HCl used, indicating the higher rate of hydrolysis and crosslinking reaction.

The results are shown more clearly in the figure 15, which displays the relationship between the ratio of Si-O-CH/ Si-O (the absorption peak at 1086  $\text{cm}^{-1}$  and 463  $\text{cm}^{-1}$ , internal reference peak) and hydrolysis time of the spiro silicate C2 at various acid concentrations at room temperature. From the mechanism proposed in Figure 12, the reactions occur during hydrolysis step are in equilibrium. Depending on acid condition, the condensation reaction may continue after hydrolysis reaction.

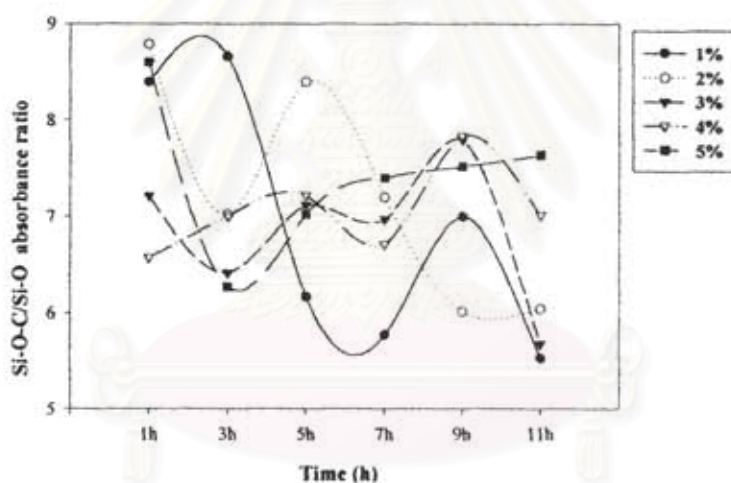


**Figure 15** The time-dependence of hydrolyzed products of spiro silicate C2 with 1%-5% of 1M HCl at room temperature.

The results indicate that the optimum condition, showing a good trend of hydrolysis sequence, is when the 1% of 1M HCl is applied, as studied by Lippert in 1988 for TEOS. Thus, this condition again was selected to apply for studying the effect of temperature, as can be seen in figure 16. It was found that at 40°C the rate of decrease of absorption peaks at 3405, 2951, 2883, 1086 and 883  $\text{cm}^{-1}$  was much faster than at room temperature.

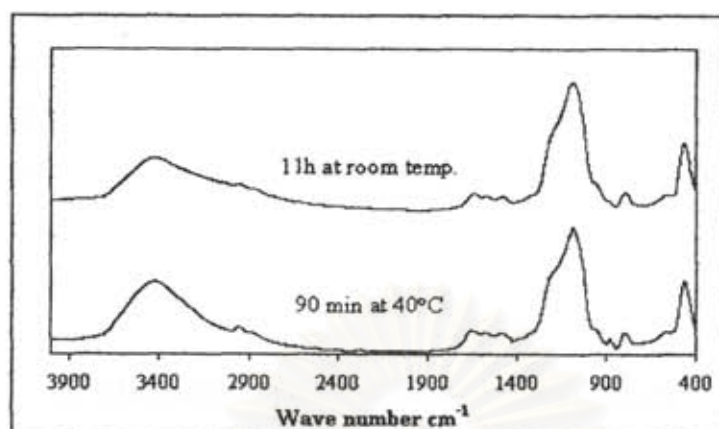


**Figure 16** FTIR spectra showing the effect of temperature on the hydrolyzed Product at room temperature and 40 °C.

Using 1M ammonium hydroxide solution

Figure 17 shows dependence of the Si-O-C/Si-O-Si absorption peak ratio versus hydrolysis time for different concentration of  $\text{NH}_4\text{OH}$ . From figure 16, for 1% of 1M  $\text{NH}_4\text{OH}$ , the results of the structural change from Si-O-C to Si-O-Si showed little change, as compared to that between spiro-silicate and hydrolyzed product, during the time period of 1 and 8 h. After 9 h, a substantial decrease of the peak ratio was observed. Subsequently, however, after 11 h, the ratio increased again. Similar to acid-catalyzed hydrolysis, the reactions during hydrolysis step are reversible, thus depending on how strong the base solution is, the reaction rate is different.

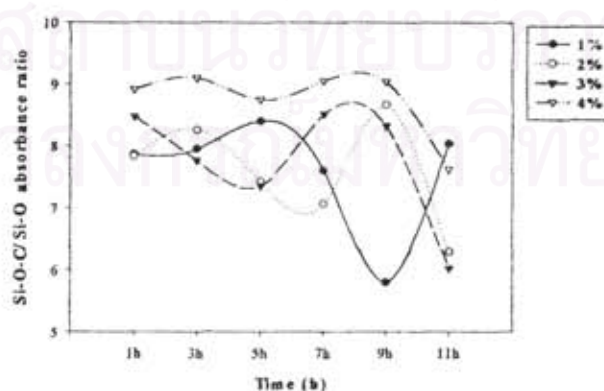


**Figure 17** The time-dependence of hydrolyzed products of spiro-silicate C2 with 1%-4% of 1M  $\text{NH}_4\text{OH}$  at room temperature.

In summary, the kinetics of the sol-gel transition of spiro-silicate C2 are the slowest at 1% and 2% of 1 M HCl, due to the absence of ionized hydroxyl groups [Si-O<sup>-</sup> or Si-(OH<sub>2</sub>)<sup>+</sup>] (LaCourse 1988), for which pH ≈ 2 (Table 3), as monitored by decrease of absorption peaks at 3405, 2951, 2883, 1086 and 883 cm<sup>-1</sup>, consistent with experimental studies of Brinker and coworkers (Brinker, 1990), who determined the optimal gel time of TEOS to be at pH near 2.

**Table 3** The pH results of different catalyst concentration.

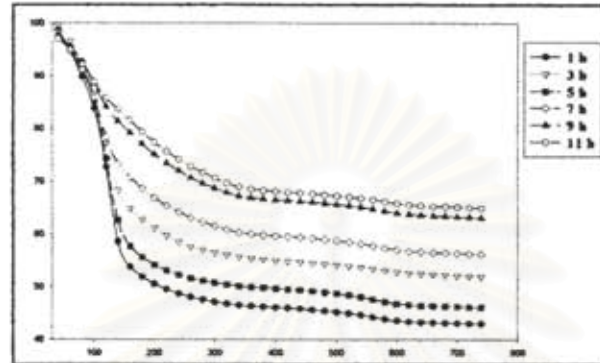
Concentration of HCl (1M)	pH result	Concentration of NH <sub>4</sub> OH (1M)	pH result
1%	2.14	1%	9.56
2%	2.03	2%	9.67
3%	1.97	3%	9.72
4%	1.81	4%	9.80
5%	1.73	5%	10.1
15%	0.65	15%	10.2

#### Thermogravimetric Analysis (TGA)

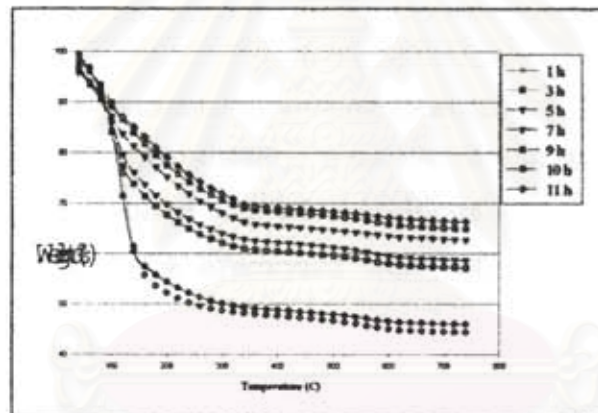
The TGA results of monomer after hydrolysis with 1% and 2% of 1M HCl were chosen to study due to the slow polymerization, as shown in figures 13 and 15. Those showed significant of decrease in the absorption peaks at 3405, 2951, 2883, 1086 and 883 cm<sup>-1</sup>. The ceramic yields of the product obtained from both conditions are shown in figure 18 (a) and (b) and in table 4.

Evidently, the kinetic data obtained from FTIR spectra and the ceramic yields from TGA are in agreement. A decrease in the absorption peak of Si-O-C and increase in Si-O-Si peak correlate to an increase in ceramic yield. Notably, the increase of Si-O-C peak at 9 h., as compared to 7 and 10 h. at 1% of 1M HCl, agrees with a decrease of ceramic yield from TGA.

Those results suggest surprisingly that the reaction can be proceed in the reverse direction, so called "reesterification", in which an alcohol molecule displaces a hydroxyl group to produce an alkoxide ligand and water as a by product (Brinker 1984, 1990).



(a)



(b)

**Figure 18** TGA thermograms showing percent ceramic yield at various times after hydrolysis with 1M HCl at (a) 1% and (b) 2%.

สถาบันวิทยบริการ  
จุฬาลงกรณ์มหาวิทยาลัย



**Table 4** The ceramic yields of the hydrolyzed monomer after using 1M HCl at various gel time.

Time (h)	Ceramic Yield (%)	
	1% of 1M HCl	2% of 1M HCl
3	44.34	51.92
5	58.61	46.11
7	62.68	56.21
9	57.13	63.02
10	64.86	-
11	66.29	64.88

#### *Aminospirosilicate C4*

##### Fourier Transform Infrared (FTIR) Spectroscopy

C4 Aminospirosilicate is 6-membered ring spirosilicate. The rings are more stable than 5-membered ring C2 spirosilicate. Moreover, C4 spirosilicate is bulkier. As the result, C4 hydrolyzed with 1M HCl and NH<sub>4</sub>OH showed no differences between room temperature and 40°C. 1M HCl also showed no difference on hydrolysis even at 60°C. Figure 19 thus shows only the results of C4 hydrolyzed using 100% of 1M NH<sub>4</sub>OH at 60°C. The decrease in absorption peaks at 3405, 2951, 2883, 1086 cm<sup>-1</sup> indicate results similar to the structure of silica.

สถาบันวิทยบริการ  
จุฬาลงกรณ์มหาวิทยาลัย

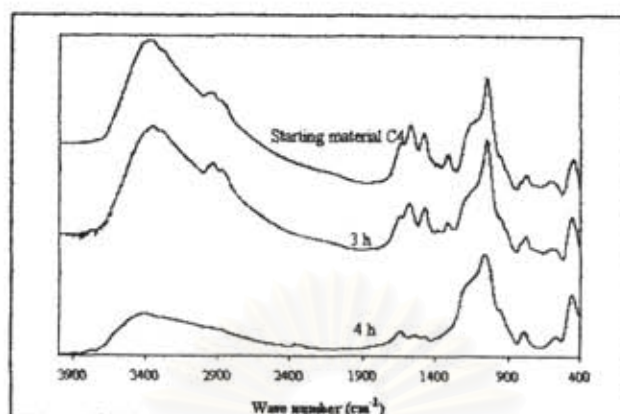


**Figure 19** FTIR spectra showing the effect of time on the hydrolyzed C4 product at 60°C.

#### Thermogravimetric Analysis (TGA)

The final ceramic yield of the polymer, hydrolyzed at 60°C for 4 h, was 70.89%, as shown in figure 20, the higher ceramic yield obtained is due to high concentration of reactive groups under base-catalyzed and high temperature resulting in less time to arrange the molecules to allow crosslinking of Si-O-Si.

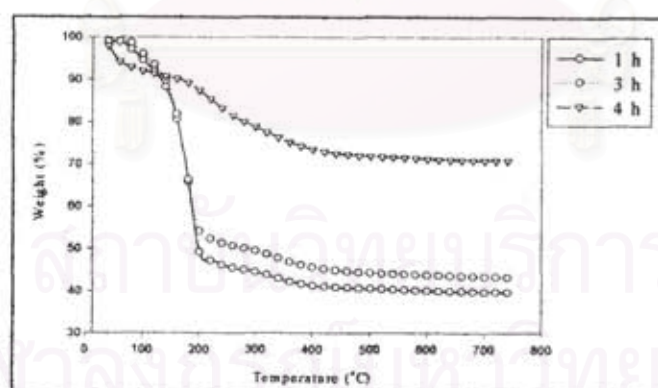


**Figure 20** TGA thermogram showing percent ceramic yield of hydrolyzed aminospirosilicate, C4 at 60°C for 1, 3 and 4 h.



#### *Characterization of Pyrolyzed Spirosilicate C2*

##### BET Surface Area Measurement

As mentioned previously that the kinetics of the sol-gel transition of spiro-silicate C2 are the slowest at 1% and 2% of 1 M HCl, due to the absence of ionized hydroxyl groups  $[\text{Si-O}^- \text{ or } \text{Si-(OH}_2\text{)}^+]$  (LaCourse 1988), for which  $\text{pH} \approx 2$  (Table 3), consistent with experimental studies of Brinker and coworkers (Brinker, 1990), who determined the optimal gel time of TEOS to be at pH near 2, the BET surface area study of pyrolyzed product obtained from hydrolyzed gel with 1 and 2% of 1M HCl at 750°C for 7 h is shown in table 5.

**Table 5** The BET surface area measurement of spiro-silicate C2 after hydrolysis with 1% and 2% of 1M HCl at various times, followed by pyrolysis at 750°C for 7 h.

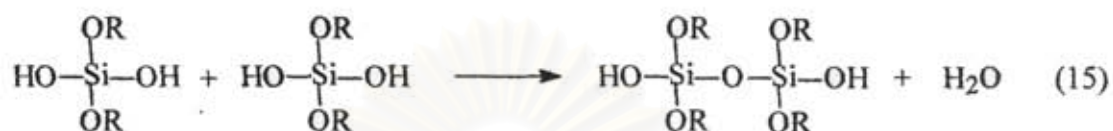
Time (hr)	Surface area ( $\text{m}^2/\text{g}$ )		Pore volume ( $\text{cc/g}$ )	
	1% of 1M HCl	2% of 1M HCl	1% of 1M HCl	2% of 1M HCl
3	448	292	0.5297	0.1811
5	458	257	0.4353	0.2380
7	524	219	0.4660	0.2040
9	561	219	0.4848	0.2148
11	598	239	0.5754	0.1895

The results from FTIR spectra, TGA and BET surface area measurements show that the decrease of  $-\text{OH}$  and  $\text{Si-O-C}$  peaks correlates to an increment of ceramic yield and surface area. Depending on the gelation time both hydrolysis and condensation rates are important to the formation of  $\text{Si-O-Si}$ . If the rates are too fast, the  $\text{Si-O-Si}$  network may collapse, resulting in less surface area. On the other hand, if the rates are too slow, TGA results will provide high ceramic yields due to the carbon residue remained in the final char.

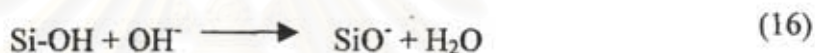
#### Scanning Electron Microscope (SEM)

The morphology of the hydrolyzed aggregates was observed by scanning electron microscopy, as shown in figure 21 (a) and (b). Each shows the

characteristics of a dried gel, under acidic and base conditions, respectively. However, certain differences in morphology are evident which can be traced to the effect of the different catalyst used. Under acid catalysis, the hydroxylated spiro-silicate is formed via electrophilic ( $H^+$ ) reaction. The condensation reaction continues via these hydroxylated spiro-silicates.



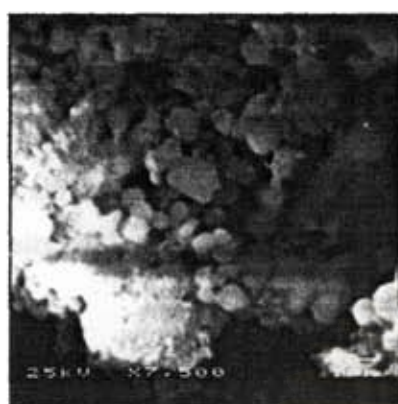
Using base catalysis, (b), the sol particles formed tend to repel each other due to a high surface charge from  $\text{SiO}^-$  groups formed according to the following reaction.



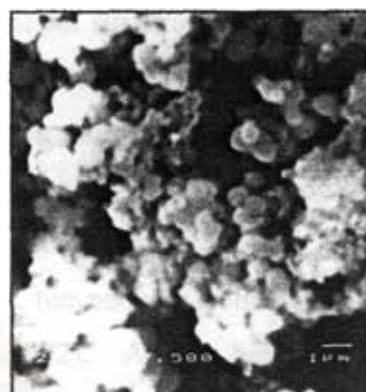
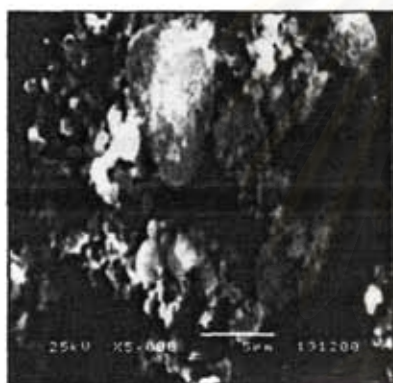
Obviously, each condition has a different influence on the rate of condensation and porosity of the dried gel product.



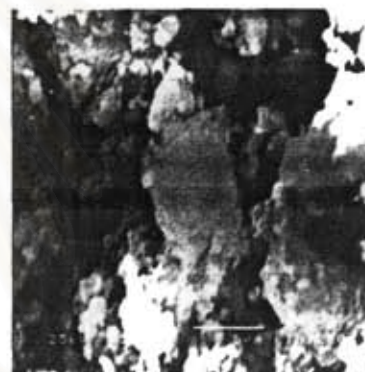
สถาบันวิทยบริการ  
จุฬาลงกรณ์มหาวิทยาลัย



(a) Hydrolysis w/ 1% of 1M HCl

(b) Hydrolysis w/ 1% of 1M NH<sub>4</sub>OH

(c) Pyrolysis of material (a) at 750°C, 7 h



(d) Pyrolysis of material (b) at 750°C, 7 h

**Figure 21** SEM of hydrolyzed (a and b) and pyrolyzed (c and d) spiro-silicate C2.

#### *Effect of Catalysts on Reaction Time*

Acid catalyst promotes the minimum reaction at 1% of 1M HCl at a pH near the iso-electric point, which gives no electrostatic particle repulsion, (near pH= 2-2.5 (Iler, 1979)). By increasing the concentration of the catalyst, the reaction rate increases, as a result, the gel time is reduced. On the other hand, the base-catalyzed reaction takes place via nucleophilic reaction (Yamane, 1988). Since the condensation reaction provides SiO<sup>-</sup>, resulting in faster condensation before completely hydrolysis.

### *Effect of Catalyst on Gel Properties*

By using base catalyst, repulsion of the sol structure gave more time for particles to rearrange. Larger particles tend to form first. This is different from using acid catalyst, occurring via addition reaction in which many small molecules tend to grow slowly (LaCourse, 1988). The SEM micrograph in figure 21 (b) shows that the porosity of the sol structure is greater than that in figure 21 (a).

In fact, the gel consists of two phase, the network solid phase and the connected pores filled with liquid phase (Ropp, 1992). As the heat treatment is applied, the gel shrinks under capillary force as the liquid evaporates. It can be seen in figure 21 (a). The HCl catalyzed gel contains small pores. If it originally contains a large amount of water molecules in the pores, upon heating the gel, the water generated from the concentration of hydroxyl groups will lead to a higher shrinkage of the gel, figure 21 (c). On the other hand, the  $\text{NH}_4\text{OH}$  catalyzed gel contains large pores and small amount of water molecules, smaller shrinkage occurs.

### Wide angle X-Ray Diffractometer (WXR)

Figure 22 shows the XRD patterns of pyrolyzed monomer, as compared to fused silica. The resulting diffraction patterns consist of a broad featureless band, showing the non-crystalline amorphous solid form.

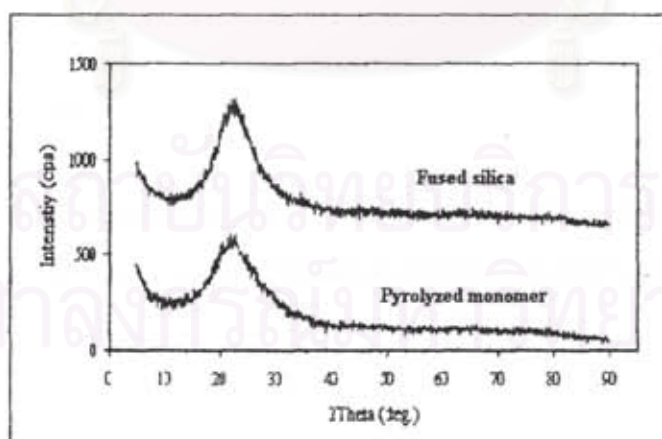


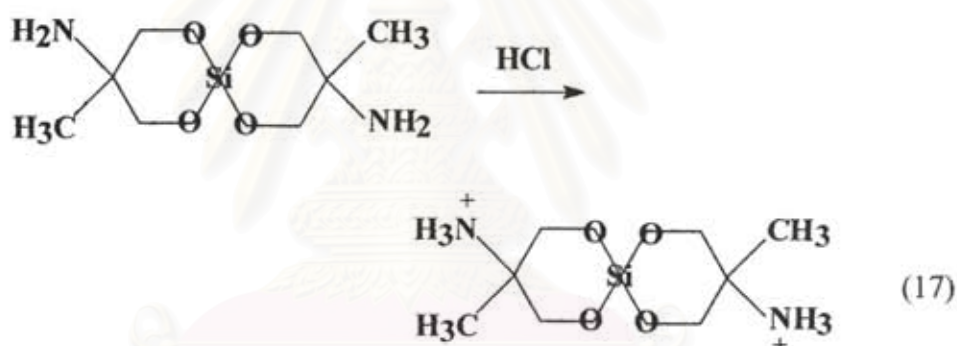
**Figure 22** XRD patterns of pyrolyzed monomer and fused- silica.

### *Characterization of Pyrolyzed Aminospinosilicate C4*

#### BET Surface Area Measurement

The BET surface area analysis of aminospinosilicate, C4 pyrolyzed products at 750°C for 7 h was 82.93 m<sup>2</sup>/g, reflecting the increase of reaction rate because of the increase in concentration of catalyst and temperature (LaCourse, W.C.,1988).

That is, under acidic condition, protonation of alkoxy group is retarded due to the more stable ring structure, more steric hindrance, and the presence of amino group in the structure, as compared to spinosilicate C2. Proton species protonated those amino group to form salts. This results in no structural change during hydrolysis of the products under acid condition, as shown in following reaction



#### *Density Measurement*

The density measurement of product obtained from hydrolyzed gel using 1% HCl of 1M gave a density value less than fused silica, as shown in table 6.

**Table 6** The density measurement of pyrolyzed product: C2 and fused silica (starting material).

Type of products	Density value (g/cm <sup>3</sup> ) at 25°C
C2	0.54
Fused-silica	2.42

The density of hydrolyzed monomer C2 was lower than fused silica due to the fact that the removal of alkoxy and hydroxyl groups by condensation reaction when the gel was heated, causes a large weight loss, produces new crosslinks and stiffening the structure. In the case of fused silica, a network structure has only small hydroxyl groups on the surfaces thus there is not significant effect on the stiffness of the structure (George, 1989).

สถาบันวิทยบริการ  
จุฬาลงกรณ์มหาวิทยาลัย



## CONCLUSIONS

Spirosilicates used for the sol-gel method can function via the reactive metal aloxide group. They are chemically produced at room temperature or slightly elevated temperature. At pH near 2, the IEP of silica particle, the products give high ceramic yields and high surface area, which is required in ceramic precursor processing. The low density property of materials was reported to be an important factor of the sol-gel method.

In addition, aminospirosilicate can serve as the starting material for study of the sol-gel transition. Because of the high stability and the steric hindrance of the extent of substitution on the structure, one needs a higher concentration and higher temperature. The product with high ceramic yield and less shrinkage can be employed to use for engineering industry applications.



สถาบันวิทยบริการ  
จุฬาลงกรณ์มหาวิทยาลัย

## REFERENCES

- Bradley, D.C., Mahotra, R.C., and Gaur, D.P. (1978). Metal Alkoxides. London: Academic Press.
- Brinker, C.J., Keefer, K.D., Schaefer, D.W., Assink, R.A., Kay, B.D., and Ashley, C.S. (1984). Sol-gel transition in simple silicates II. Journal of Non-Crystalline Solids 63, 45-59
- Brinker, C.J., and Scherer, G. W. (Eds.). (1990). Sol-Gel Science: The Physics and Chemistry of Sol-Gel Processing. San Diego: Academic Press.
- Brinker, C.J., Bunker, B.C., Tallant, D.R., Ward, K.J., and Kirkpatrick, R.J. (1988). Structure of sol-gel-derived inorganic polymers: silicates and borates. In Martel, Z., Kenneth, J.W., and Harry, R.A., (Eds.). Inorganic and Organometallic Polymers: Macromolecules Containing Silicon, Phosphorus, and Other Inorganic Elements. Washington D.C.: American Chemical Society.
- Charles, D.E., Payne, D.A., and Payne, L.A. (1994). Sol-Gel Processing of electrical and magnetic ceramics. Materials Chemistry and Physics, 38, 305-324.
- Charoenpinikarn, W., Suwankuruhasn, M., Kesapabutr, B., Wongkasemjit\*, S. and Jamieson, A. M. (2001). Sol-gel processing of silatranes. European Polymer Journal, 37/7, 1441-8.
- Clarson, S.J., and Semlyen, J.A. (Eds.). (1993). Siloxane Polymers. New Jersey: PTR Prentice Wall.
- David, A., Ward, I.K., and Edmond, I. K. (1995). Preparing catalytic materials by the sol-gel method. Ind. Eng. Chem. Res., 34, 421-433.
- Iler, R.K. (1979). The chemistry of Silica. New York: Wiley.
- James, E.M., Harry, R.A., and Robert, W. (Eds.) (1992). Inorganic Polymers. New Jersey: Prentice-Hall International.
- Jung, K.Y., and Park, S.B. (2000). Enhanced photoactivity of silica-embedded titania particles prepared by sol-gel process for the decomposition of trichloroethylene. Applied Catalysis B: Environmental, 25, 249-256.

- LaCourse, W.C. (1988). Continuous filament fibers by the sol-gel process. In Lisa C. K. (Ed.). Sol-Gel Technology for Thin films, Fibers, Prefroms, Electronics, and Specialty Shapes. New Jersey: Noyes Publication.
- Lippert, J.L., Melpolder, S.B., and Kelts, L.M. (1988). Raman spectroscopic Determination of the pH dependence of intermediates in sol-gel silicate formation. Journal of Non-Crystalline Solids, 104, 139-147.
- Livage, J. (1989). Sol-gel chemistry of transition metal oxides. In Aegerter, M.A., Jafellicci Jr., M., Souza D.F., and Zanotto, E.D. (Eds.). Sol-Gel Science and Technology. Singapore: World Scientific.
- Mackenzie, J.D. (1986). Applications of the sol-gel method: some aspects of initial processing. In Hench, L.L., and Ulrich, D.R. (Eds.). Science of Ceramic Chemical Processing. Canada: John Wiley & Sons.
- Mahotra, R.C., (1989). Metal alkoxides and their derivatives with carboxylic acids and  $\beta$ -diketones as precursors in solution-sol-gel process. In Aegerter, M.A., Jafellicci Jr., M., Souza D.F., and Zanotto, E.D. (Eds.). Sol-Gel Science and Technology. Singapore: World Scientific.
- Ropp, R.C. (1992). Studies in Inorganic Chemistry 15: Inorganic Polymeric Glasses. Amsterdam: Elsevier
- Varangkana Jitchum, Chivin Sun, Sujitra Wongkasemjit\* and Hatsuo Ishida (2001). Synthesis of spiro-silicates directly from silica and ethylene glycol/ethylene glycol derivatives. Tetrahedron, 57(18), 3997-4003.
- Turgay, S., Bekir, C., and Ismail, O. (2000). Sol-gel synthesis of Ru(II) complex of 3-4,5-dihydroimidazol-1-yl-propyltriethoxysilane aerogels and xerogels. Polymer Bulletin, 44, 47-53.
- Turner, C.W., and Franklin, K.J.(1986). A Multinuclear ( $^1\text{H}$ ,  $^{29}\text{Si}$ ,  $^{17}\text{O}$ ) NMR study of the hydrolysis and condensation of tetraethylorthosilicate (TEOS). In Hench, L.L., and Ulrich, D.R. (Eds.). Science of Ceramic Chemical Processing. Canada: John Wiley & Sons.
- Yamane, M. (1988). Monolith formation from the sol-gel process. In Lisa C., and Klein. (Eds.). Sol-Gel Technology for Thin Films, Fibers, Prefroms, Electronics, and Specialty Shapes. New Jersey: Noyes Publication.